https://doi.org/10.15407/ufm.21.01.102

**O.B. LYSENKO [1], I.V. ZAGORULKO [2,*], and T.V. KALININA [1]**

[1] Dniprovsky State Technical University,
Dniprobudivska Str., 2, UA-51918 Kamianske, Ukraine

[2] G.V. Kurdyumov Institute for Metal Physics of the NAS of Ukraine,
36 Academician Vernadsky Blvd., UA-03142 Kyiv, Ukraine

# CONDITIONS FOR THE FABRICATION OF METALLIC GLASSES AND TRULY AMORPHOUS MATERIALS

A review of the literature data on the problem of the disordered structural-states' formation during the rapid cooling of metallic melts is performed. The author's approach novelty consists in the fact that, in addition to the generally accepted model of metallic glasses (MG), which are structurally amorphous–nanocrystalline composites, the conditions for fixing single-phase amorphous structures lacking inclusions of the crystalline component are analysed. The criteria for the tendency of melts to noncrystalline solidification are considered: 'deep eutectic', thermodynamic, structural (topological), physicochemical, and kinetic ones. Particular attention is paid to the works, in which the critical values of the thickness and cooling rate of melts providing the MG formation are defined through a consistent solution of thermal and kinetic problems formulated regarding the quenching from the liquid state (QLS) process. As shown, using the model of effective rates of nucleation and crystals' growth in studies of mass-crystallization kinetics allows analysing the complex transformations, which occur under conditions of competition between several crystalline phases and/or transformation mechanisms, and simplifies the calculations of the microstructure parameters of the QLS products. The authors propose a detailed description of the thermokinetic analysis of amorphization conditions for metal melts, which is also contained in the present work. As proved, the probability of metal glasses structure formation is primarily determined by the crystal-growth rate, the value of which is controlled by the ratio of the difference between the free energies of the liquid and crystalline phases, $\Delta G_V$, to the viscosity of the melt, $\eta$. The intervals of the $\Delta G_V/\eta$ criterion values are determined for materials of four groups with significantly different vitrification ability. The final section contains the results of a computational analysis of the conditions for suppressing the nucleation

* zagorylko@ukr.net

Citation: O.B. Lysenko, I.V. Zagorulko, and T.V. Kalinina, Conditions for the Fabrication of Metallic Glasses and Truly Amorphous Materials, *Progress in Physics of Metals*, **21**, No. 1: 102–135 (2020)

processes and fixation of truly amorphous structural states. As follows from the relevant literature data, only alloys, which solidify as MG when casting into a metal mould, demonstrate the real prospect for obtaining the fully amorphous structures. As concluded, the main factors increasing the ability to absolute amorphization are relatively low (up to $10^{20}$ $m^{-3} \cdot s^{-1}$) values of the stationary frequency of crystallization-centres' formation and a pronounced tendency to retardation of the nucleation processes with increasing cooling rate of the melts.

**Keywords:** quenching from the liquid state, criteria for tendency to amorphization, metallic glasses, truly amorphous states, nonequilibrium crystallization models, crystal-growth rate, nucleation frequency.

## 1. Introduction

The first example of noncrystalline solidification of metal melts is an article [1] published in 1960, the authors of which succeeded in converting the eutectic alloy of the Au–Si system to an amorphous state. This work initiated the turbulent development of studies of different classes of rapidly quenched amorphous alloys (AA) as well as the engineering of highly efficient methods for their production. The solution of this scientific and technological problem is still relevant today, which is explained by both the high level and unique combinations of AA properties and the possibility of creating materials with a nanocrystalline structure based on them [2].

A distinctive feature of the rapidly quenched amorphous alloys structure is the absence of a characteristic for crystalline substances of long-range order in the atoms arrangement. Conclusions about the fixation of such structure are usually made based on the analysis of x-ray diffraction patterns, which contain only a few (3–4) blurred maxima. Diffractograms of liquid metals and materials with heterophase nanocrystalline structures also have a qualitatively similar character. Therefore, substances, which give diffuse diffraction patterns, are sometimes called x-ray amorphous, thus, emphasizing that the conclusion about the structural state of the material was made solely by the type of dependence of the scattered x-ray radiation intensity on the reflection angle.

To clarify the physical nature of the amorphous state, which is fixed due to the solidification of the supercooled liquid phase, consider the changes in volume $V$ at the alloy temperature $T$ decreasing [3]. As can be seen from Fig. 1, in the region of thermodynamic stability of the melt ($T > T_m$), an almost linear relationship between volume and temperature is observed. In this section of the $V(T)$ dependence, the structure of the liquid phase is continuously changed by rearranging the kinetic units, and during the cooling time, the state of internal equilibrium has time to be established in the liquid. Below the temperature $T_f$, the establishment of the equilibrium state is delayed, and when the temperature $T_g$ is reached, it practically stops. The temperature range $T_f$–$T_g$

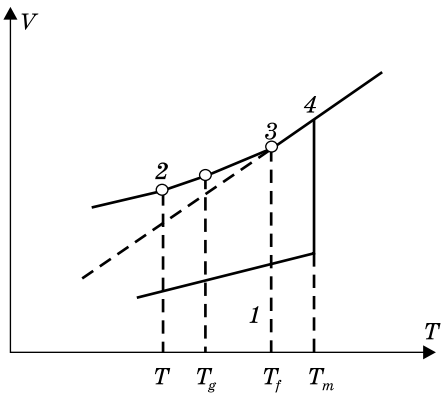


*Fig. 1.* Diagram sketch of the volume changes during the melt solidification [3]: *1* — crystalline phase, *2* — glassy phase, *3* — supercooled melt, *4* — overheated melt

is called as the glass formation interval, and the state of the material below $T_g$ is called glassy. Temperature $T_g$ corresponds to viscosity ~$10^{12}$ Pa·s. Thus, the structure of materials hardening without crystallization is fixed after the complete cessation of the rearrangement processes of atomic complexes, which set the short-range order parameters of the supercooled-liquid phase. In other words, rapidly quenched amorphous alloys inherit the melt structure corresponding to the temperature $T_g$.

Amorphous alloys have an increased free energy both relative to the equilibrium crystalline state, and in comparison with the supercooled liquid phase, which is in a state of internal equilibrium (dashed line in Fig. 1). During the subsequent heating, the structure of rapidly quenched amorphous alloys undergoes changes due to the development of devitrification processes (*i.e.*, transition from a solid amorphous state to a state of a supercooled melt), structural relaxation and crystallization.

To refer to materials, which do not have a long-range atomic order, the terms used in the literature are as follow: noncrystalline, amorphous, or glassy ones. Which of these definitions should be preferred? Reflecting on this question, I.S. Miroshnichenko [3] refers to the terminological recommendations of the Russian Academy of Sciences (RAS). According to the RAS, glasses include 'all amorphous substances obtained by supercooling of a melt, independently on their chemical composition and temperature range of the solidification, which acquire the properties of solids due to a gradual increase in viscosity; the transition process from liquid to glassy state should be reversible'. It follows that in relation to rapidly quenched products, the terms 'amorphous alloy' and 'metallic glass' (MG) are synonymous. On the other hand, noncrystalline materials obtained not from the melt, but, *e.g.*, by methods of deposition from electrolytes or vapour condensation cannot be referred to the glasses. However, all of them, including rapidly quenched metallic glasses, are amorphous materials.

For a deeper understanding of the metallic glass nature, we will answer the question of whether they are amorphous materials in a strictly structural sense. The legitimacy of raising this question is based on the peculiarities of the transition of the melts to the glassy state. Indeed, during the period of melt cooling from the melting temperature $T_m$ to

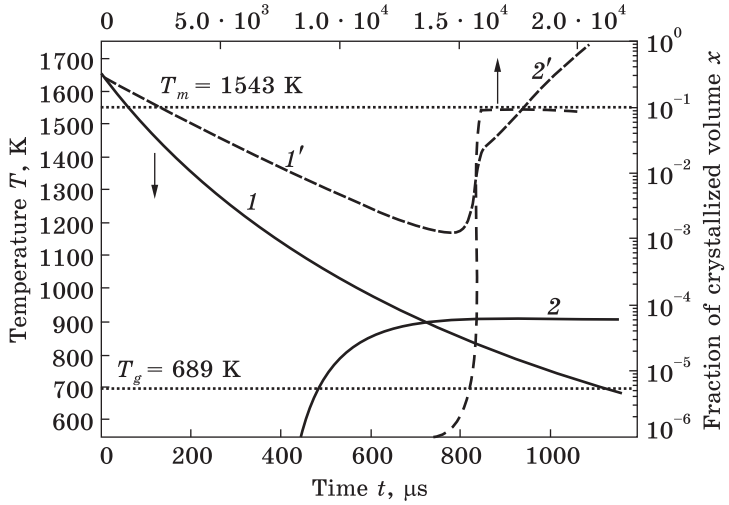


*Fig. 2.* Calculated time ($t$) dependences of temperature $T$ (*1*, *1′*) and fraction of the crystallized volume $x$ (*2*, *2′*) for $Fe_{80}B_{20}$ alloy layers of 20 μm (*1*, *2*) and 100 μm (*1′*, *2′*) thick [7]

the glass transition temperature $T_g$, there are thermodynamic prerequisites for the development of crystals nucleation and growth processes. According to computational analysis [4–8], the degree of implementation of these processes, therefore, the structure of rapidly quenched materials, depends on the ratio of heat fluxes, one of which ($Q_1$) is discharged into the refrigerator, and the other ($Q_2$) is released in a solidifying bulk as hidden heat of transformation.

If $Q_1 < Q_2$, then, after the formation of the crystalline-phase volume fraction of ~$10^{-2}$, the melt temperature rises sharply and the main stage of the process is carried out with slight supercooling relative to $T_m$, which corresponds to high values of the crystal growth rate. Under these conditions, the fast quenching products acquire the fully crystallized microcrystalline structure (dashed curves in Fig. 2). With the inverse ratio of heat fluxes ($Q_1 > Q_2$), the melt temperature continuously decreases. During the cooling time from $T_m$ to $T_g$, a certain number of crystallization centres are formed in the melt, the growth rate of which is negligible at deep supercooling. As a result, a structure typical for metallic glasses is fixed. It consists of an amorphous matrix with inclusions of the so-called 'quenched nuclei' (solid curves in Fig. 2).

The presence of nanoscale crystallization centres in the MG structure is confirmed by the data of transmission electron microscopy (TEM) [9–11] and the results of model studies of the nonequilibrium crystallization kinetics [6–8, 12, 13], but practically it does not affect the character of x-ray diffraction patterns. The total number of 'quenched nucleus' per unit volume (up to ~$10^{17}$–$10^{18}$ $m^{-3}$), their sizes (up to 10 nm)

and volume fraction (up to $10^{-2}$) depend on several factors. They are the cooling regime of the melt, the values of thermodynamic and kinetic parameters, which specify the crystals nucleation and growth rates, on the magnitude of the temperature range $T_m - T_g$, and some other factors. Particularly, the structural analysis of the $Cu_{60}Ti_{10}Zr_{30}$ alloy, which was obtained in the form of 2.5 mm diameter rods by casting into a copper mould, and thin (30 μm) ribbons by melt spinning, was performed in [11]. It is shown that both the rods and ribbons of the investigated alloy have a typical for MG structure, the elements of which are a glassy matrix and nanoscale inclusions of the crystalline phase, and the volume fraction and the size of nanocrystals in ribbons are reduced in comparison with rods. Based on these experimental data, the authors of [11] concluded that a single-phase amorphous state could be fixed in the $Cu_{60}Ti_{10}Zr_{30}$ alloy under conditions of higher cooling rates. However, any evidence of this conclusion is not given.

Thus, according to the results of numerous theoretical and experimental studies, rapidly quenched metal glasses have a two-phase structure, *i.e.*, in fact, they are amorphous–nanocrystalline composites [14] or conditionally amorphous materials. At the same time, in the literature, there are some publications where authors report about the production of completely amorphous structures that do not contain 'quenched nuclei'. For example, a similar structure was observed by the TEM method in the contact areas of rapidly cooled ribbons of the $Fe_{80}B_{20}$ alloy with a thickness of 40 μm [10]. According to data [15] obtained by summarizing the results of x-ray phase analysis, electron diffraction and TEM, rapidly quenched ribbons of $Al_{85}Ni_5Y_8Co_2$ alloy about 20 μm thick demonstrate a single-phase disordered structure without any signs of nanocrystals or ordered clusters, which, in the authors' opinion, demonstrate the fully glassy state of the samples. The disagreements noted in the literature data do not give an unambiguous answer to the question regarding the fundamental possibility and technological regimes of obtaining truly amorphous states. Consequently, the problem under consideration remains relevant and requires solving by analysing the factors that determine the glass-forming ability (GFA) of materials, as well as studies of the structure formation process during the rapid cooling of metal melts.

## 2. Criteria for the Tendency of Melts to Noncrystalline Solidification

One of the most important directions of the study of the effect of metal melts amorphization is an establishment of correlations between the chosen from physical considerations materials characteristics and the conditions for production of this materials in a noncrystalline state.

They make it possible to identify the factors that control the predisposition of melts to the glass transition, and facilitate the search for compositions of new MG.

Since the first amorphous phase was fixed in the eutectic alloy $Au_{75}Si_{25}$, this feature of the state diagram was used as the basis for the choice of other alloys, which were amorphized during quenching from the liquid state [16–18]. The physical aspect of this approach is that the eutectic temperature is the minimum temperature stability of the liquid phase. Consequently, the cooling time from this temperature to the temperature $T_g$ will also be minimal. Moreover, the lower the eutectic temperature relative to the melting points of the eutectic phases, *i.e.*, the 'deeper' the eutectic, the easier the melt should be amorphized. With the help of the 'deep eutectic' criterion, the amorphous state was fixed in a sufficiently large number of rapidly quenched alloys, including alloys based on light rare-earth elements (La, Ce, Pr, …) with normal (Al, Ga, Cu, Ag, …) and transitional (Ni, Co, …) metals [19].

The main disadvantage of this criterion is the possibility of using only for a limited number of binary or ternary alloys with known state diagrams. In addition, according to the results of experimental studies, not all eutectic alloys demonstrate the greatest ability to glass transition. It was also established that in some alloys (*e.g.*, Cu–Zr, La–Al, *etc.*), amorphous phases are fixed at ratios of components that belong to the regions of equilibrium intermetallic compounds existence. These circumstances stimulated the search for other approaches to predict the propensity of alloys to noncrystalline solidification under the conditions of QLS, within which thermodynamic, topological (or structural), physicochemical, and kinetic criteria for amorphization were created.

The thermodynamic criteria are based on the ratios of melting temperatures $T_m$, transition to the glassy state $T_g$, and the crystallization of the amorphous phase upon heating $T_x$, which are determined by the methods of thermal analysis and differential scanning calorimetry. The simplest and most widely used criterion of this group is the reduced glass transition temperature $T_{rg} = T_g/T_m$. The physical substantiation of this criterion is that the melts crystallize in the temperature range $T_m$–$T_g$. Consequently, all factors that reduced this interval, *i.e.*, increase $T_g$ and reduce $T_m$, should promote noncrystalline solidification of materials.

For currently known metallic glasses, $T_{rg}$ values range changes from 0.246 (for Ni) to 0.690 (for $Pd_{40}Cu_{30}Ni_{10}P_{20}$ alloy) and, as a rule, correlate with critical cooling rates $\upsilon_c$ sufficient for amorphization, which for the given examples are ~$10^{10}$ and $10^{-1}$ K/s, respectively. However, when analysing the relative propensity for amorphization of so-called bulk metallic glasses, for which the value $\upsilon_c$ is determined quite accurately, the $T_{rg}$ criterion is less effective [20].

Instead of the reduced glass transition temperature $T_{rg}$, other criteria have been proposed. It represents different combinations of $T_m$, $T_g$, and $T_x$. In particular, among them there is the temperature difference $\Delta T_{xg} = T_x - T_g$, which characterizes the stability of supercooled melts in the crystallization process [18]. The parameters being tested are as follow:

$$\gamma = T_x/(T_g + T_m),\ \gamma_m = (2T_x - T_g)/T_m,$$
$$\Delta T_{rg} = (T_x - T_g)/(T_m - T_g),\ \delta = T_x/(T_m - T_g),$$

*etc.* A comparative analysis of the effectiveness of these criteria, carried out by the authors of papers [21, 22], showed that the parameter $\gamma_m$ should be considered the most correct of them. However, despite a certain correlation of most thermodynamic criteria with the tendency of alloys to amorphization, as well as the establishment of a direct connection of some of them with a critical cooling rate (for example, $\upsilon_c = 5.1 \cdot 10^{21} \exp(-117.19\gamma)$ [22]), all of them have limited applicability only for some alloys classes. In addition, a common disadvantage of thermodynamic criteria is their unsuitability for predicting the conditions of noncrystalline solidification, since their parameters $T_g$ and $T_x$ are determined by heating amorphous alloys.

Structural or topological criteria are devoid of the latter deficiency [23–27]. In these criteria, the atomic dimensions of the components and the density of their packing are analysed. The structural approach is based on the Egami assumption reported in Ref. [23], according to which the tendency of melts to amorphization increases if the level of local mechanical stresses caused by differences in the atomic sizes of the main and alloying elements exceeds a certain critical value, which causes a loss of the topological stability of the crystal lattice. Based on these considerations, the author of [23] obtained the relationship between the minimum content of the alloying element $C_B^{\min}$, which provides the amorphization of the binary alloy, and the atomic radii of the components $r_A$ and $r_B$:

$$C_B^{\min} = 0.1/|(r_B/r_A)^3 - 1|\,. \qquad (1)$$

Expression (1) is simple and convenient to use. However, an attempt to use it to assess the propensity for noncrystalline solidification of binary aluminium with rare-earth metals alloys [28] showed that the analysis of only the atomic dimensions of the components is insufficient. According to Ref. [24], the reason for the low efficiency of the Egami criterion is that it does not take into account possible arrangements of the atoms of the alloying element in the lattice of solvent element. In fact, in complex alloyed alloys, small-sized atoms can not only replace the base metal atoms in the lattice sites, but also occupy penetration positions in tetra- or octahedral pores, and causes a complication of the stress field. In particular, in alloys based on zirconium, palladium and rare-earth metals, in which the atoms of the alloying elements, as a rule,

have smaller sizes in comparison with the atoms of the main component, the implanted atoms create the positive stresses in the lattice, while the stresses formed in the positions substitutions has a negative sign.

The complex nature of field of local mechanical stresses in the volume of multicomponent alloys is taken into account in the model [25–27]. It allows to analyse the distribution of atoms of alloying elements between the substitution and insertion positions as a function of the lattice strain energy as well as to determine the ratio of atomic sizes and component concentrations that provide a high local packing density of atoms, and, consequently, increase the susceptibility of melts to amorphization.

To test the effectiveness of an improved topological approach, the authors of [29] selected 16 calcium-based alloy compositions that should form bulk metallic glasses. However, according to experimental data, only 7 alloys were transferred into an amorphous state in castings with a thickness of 1 mm. In addition, experimental estimates of the critical cooling rate of multicomponent iron-based alloys have shown that variations in the relative amounts of transition elements present in the composition, which have similar atomic dimensions, are accompanied by significant changes in the glass-forming ability [30]. These facts indicate that the topological criteria have limited applicability for predicting the propensity of materials to noncrystalline solidification.

For the choice of alloys that are amorphized under the QLS conditions, the physicochemical approach is more productive. It takes into account not only the atom characteristics of the components, but also the features of their interaction. Developing this approach, the authors of the monograph [16] identified three groups of physicochemical factors following below.

(1) Characteristics of state diagrams: the presence of relatively narrow regions with low melting temperatures. The physical substantiation of this requirement is given above in the analysis of the criterion of 'deep eutectic'.

(2) Physical and chemical properties of the components:

• significant differences in the atomic radii of the components ($r_A/r_B$ = 0.79–1.41);

• valence difference $\Delta n$ of elements included in the composition of the alloys: $\Delta n$ = 3–5 for transition metal with non-metals alloys and $\Delta n$ = 5–6 for alloys of different transition metals (an analysis of the effectiveness of the considered factor using the example of a large number of alloys based on light lanthanides showed that a certain $\Delta n$ value is not a necessary condition for melt amorphization [19], moreover, for alloys with the same component valence (*e.g.*, Mg–Zn), the $\Delta n$ criterion loses meaning);

• the difference in electronegativity: for the majority of amorphized alloys, the value of this parameter varies from –0.3 to 0.2, howe-

ver, its actual role in the formation of the MG structure is not fully understood;

• position in the periodic system of elements: components, which contribute to amorphization when interacting with this element, are characterized by a general tendency to be located in different parts of the periodic table so that the corresponding properties differ, but not too much.

(3) Features of equilibrium and metastable phases crystallizing at subcritical cooling rates of melts:

• predisposition of alloys to the formation of intermediate phases with a complex crystalline structure, such as the Frank–Kasper phases (σ, μ phases, and Laves phases), as well as $Fe_3C$-type phases: according to [16, 31], the tendency of melts to glass formation increases, if concentration ranges of amorphization under equilibrium conditions or under conditions of QLS with cooling rates which are insufficient for non-crystalline solidification, crystalline phases of these types are formed, although in some alloys (for example, on the basis of light REM with silver and aluminium) the amorphous state is fixed due to the crystallization suppression of the metastable phase of the initial composition with a b.c.c.-lattice [19, 32, 33];

• mechanism of eutectic phases crystallization: as shown in [34], the tendency of melts to amorphization increases if the phases involved in eutectic transformations belong to incongruent compounds, *i.e.*, formed by peritectic reactions, which are characterized by low rates;

• concentration of valence electrons: using the approximation of almost free electrons, the authors of [35] showed that the glass-forming ability of alloys depends on the value of electron concentration, reaching a maximum level at $e/a \approx 2$ el./at. (in fact, in alloys of different classes, the optimal value $e/a$ for amorphization varies from ≈1 el./at. (Pd–Si) to ≈5–7 el./at. (Nb–Ni)).

The physicochemical criteria proposed in [16] were later significantly modified by reducing the list of analysed parameters and focusing on the indicators of the total number of components and the nature of their interatomic interaction. According to the improved version of the physicochemical approach [18], alloys, which demonstrate an increased tendency to glass transition, should satisfy three requirements: contain at least 3 components (1); characterized by significant (≥12%) differences in atomic size (2) and negative values of the heat of mixing of the components (3). The listed conditions turned out to be useful for the search of new amorphized alloys. In particular, with their help, several groups of alloys based on Zr, Pd, Fe, and lanthanides were discovered. The crystallization of this alloys is suppressed at relatively low (up to 0.01 K/s for $Pd_{40}Cu_{30}Ni_{10}P_{20}$ alloy) cooling rates of the melt [18].

By additional studies of the interrelationships of the criteria proposed in [18] with a critical cooling rate $\upsilon_c$, which provided the glassy

solidification of the melt, it was found that increasing the differences in the atomic sizes of the components over 12% leads to a decrease of $\upsilon_c$ on one or two magnitude orders, while increasing of the absolute value of negative heat mixing is accompanied by a more significant (from $10^3$ to $10^7$ times) decline of $\upsilon_c$ values [36]. Based on the results of the performed analysis, the physicochemical criteria for the tendency of alloys to amorphization were rethought and formulated in Ref. [36]: alloys must possess the heat of mixing not less than –15 kJ/mole and excessive melting entropy $S_\sigma/k_B$, which are exceeds 0.1 at a packing density of 0.64.

Despite periodically undertaken attempts to improve the physicochemical criteria, they are not mandatory for relatively easy amorphization of materials. In particular, the requirements of the multicomponent content and the proximity of the composition to the eutectic are not fulfilled for the $Cu_{64.5}Zr_{35.5}$ alloy, which is obtained in the amorphous state in the form of rods with a diameter of 2 mm by melt casting into a copper mould [37], and in a number of easily amorphized alloys the phase separation was found [38, 39], which indicates a positive enthalpy of mixing the components.

Analysing the totality of the above requirements for alloys passing into the glassy state under the conditions of QLS, we note that some criteria (*e.g.*, proximity to low-temperature eutectic compositions as well as significant differences in atomic size) are used not only as self-sufficient critical parameters, but also in as one of the conditions of physicochemical approaches [16, 18] or an element of the hybrid criterion, among which the parameter σ which was proposed for predicting glass formation in ternary systems [40].

This criterion is a combination of the structural criterion by Egami [23], modified for ternary alloys, and reduced supercooling as remarked by Donald and Davies [41]. A comparative analysis of the glass-forming ability of a group of ternary alloys based on Ca, Mg, Pd, Zr, La, and Nd, performed by the authors of [40] using the parameter σ, showed that it correlates well with the experimental values of the sections of amorphized ingots. However, the hybrid criterion σ was tested on the example of only ten three-component alloys, which form metallic glasses in sections from 2 to 15 mm. Therefore, it needs further modification and efficiency testing for a wide range of multicomponent alloys.

A common disadvantage of the above thermodynamic, structural and physicochemical criteria for the tendency of materials to amorphization is that they do not consider the mechanisms of glassy solidification under the QLS conditions. This problem is solved using the kinetic approach, which was first proposed by Uhlmann [42] and was further developed in the works of Davies (see Ref. [17] and several chapters in Ref. [43]). Within the scope of this approach, the glass-forming ability

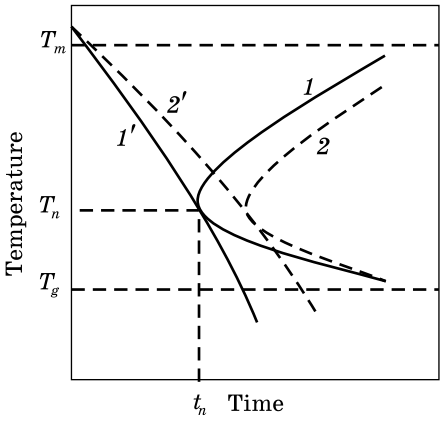


*Fig. 3.* Schemes of TTT diagrams (*1*, *2*) and dependences $T = T(t)$ (*1′*, *2′*), corresponding to the critical speed of QLS, where *1* — isothermal conditions, *2* — transformation with continuous cooling

of materials correlates with the critical rate $\upsilon_c$ of quenching from the liquid state. During the quenching, the entire cooling time of the melt only an insignificantly small (not detected experimentally) volume fraction of the crystalline phase $x_e$ is formed, which corresponds to the limits of the sensitivity of electron microscopic (~$10^{-6}$ [42, 43]) and x-ray phase (~$10^{-2}$ [44]) analyses.

To implement kinetic calculations by simplifying transformations of the classical theory of crystallization equations, an approximate relation for time intervals, during which a given of crystallized volume fraction $x_e$ is formed at various supercoolings of the melt, was derived:

$$t_{x_e}(T) \approx \frac{9.3\eta}{k_B T}\left\{\frac{x_e a_0^9}{f^3 N_V}\left[\exp\left(\frac{1.07}{T_r^3 \Delta T_r^2}\right)\right]\left[1-\exp\left(-\frac{\Delta H_m \Delta T_r}{RT}\right)\right]^{-3}\right\}^{1/4}, \quad (2)$$

where $T$ — melting temperature, $\eta$ — dynamic viscosity, $k_B$ — Boltzmann constant, $f$ — the fraction of positions at the melt/crystal interface at which atoms can attach ($f = 1$ for rough and $0.2\Delta T_r$ for smooth interfaces), $N_V$ — number of atoms per unit volume, $T_r$ and $\Delta T_r$ —reduced temperature ($T/T_m$) and supercooling ($1 - T_r$), respectively, $\Delta H_m$ — molar heat of fusion, $R$ — universal gas constant.

The values $t_{x_e}$ calculated at various temperatures are summarized in the form of 'time–temperature-transformation (TTT)' diagrams, which have the form of C-shaped curves (Fig. 3) and allow us to estimate the minimum (critical) cooling rate $\upsilon_c^{x_e}$, which provides glassy solidification of the melt with the formation of a negligible volume fraction of crystalline phase $x_e$.

The $\upsilon_c^{x_e}$ value is determined by the tangent of the angle of drawn from the initial temperature of the melt to the point of protrusion ('nose') of the TTT diagram (lines 1′ and 2′ in Fig. 3) according to the relation [43]:

$$\upsilon_c^{x_e} \approx (T_m - T_n)/t_n, \quad (3)$$

where $T_n$ and $t_n$ — temperature and time corresponding to the point of minimum stability of the supercooled melt.

As analysis [36, 43, 45] showed, the critical cooling rates determined by the considered above method correctly reflect the relative tendency

to amorphization of various alloys, however, they are consistent with experimental data within the same order of magnitude. To increase the accuracy of forecasts, it is necessary to take into account the nonisothermal character of crystallization process at quenching from the liquid state [43], which leads to a shift of the C-shaped curves toward longer time intervals (curve *2* in Fig. 3) and a corresponding decrease in the $\upsilon_c^{x_e}$ value. Despite the noted drawbacks, the method of constructing TTT diagrams has been used for many years to analyse the amorphization conditions of metals and alloys, including the production of bulk metallic glasses [46–48].

A physically more rigorous formulation of the problem associated with the study of the kinetics of nonequilibrium crystallization from the liquid and amorphous phases is based on the use of algorithms for the coordinated numerical solution of the heat equations for the melt and the refrigerator with the equation of the mass crystallization kinetics [8, 12, 13, 49, 50]. An important advantage of this approach is the possibility of a comprehensive analysis of the thermal and kinetic aspects of the amorphization process. As the kinetic component of the model in works [12, 13, 49], it is the classical equation by A.N. Kolmogorov [51], which sets the dependence of the crystallizing volume fraction on time:

$$x(t) = 1 - \exp\left\{-\frac{4}{3}\pi\int_0^t I(t')\left[\int_{t'}^t u(t'')dt''\right]^3 dt'\right\}, \qquad (4)$$

where $I$ and $u$ are nucleation frequency and crystal growth rate, respectively.

Equation (4) is derived in relation to the process of crystallization from a melt of one phase, which is carried out by the homogeneous formation of crystalline nuclei and their further isotropic growth. These statements make it difficult to apply Kolmogorov-type equations for more difficult transformations occurring under conditions of competition between several crystalline phases or various crystallization mechanisms. In addition, in the framework of the model by A.N. Kolmogorov, it is very difficult to calculate the most probable crystal sizes [52, 53], which are the most important microstructural characteristic of materials.

## 3. Applying the Model of Effective Rates of Nucleation and Crystal Growth in the Studies of the Mass Crystallization Kinetics

To overcome the noted kinetic limitations, a different version of the kinetic analysis of mass crystallization was proposed in [54]. In this approach, the increment of the crystallizing volume fraction $dx$ in an

elementary time interval $dt$ is determined through the relative contributions of the nucleation and growth processes, which are caused by the appearance of a certain number $dN$ of nuclei with critical size $R_c$ and an increase in the linear dimensions $dR$ of all currently available crystals. It is assumed that under constrained conditions of mass crystallization, the values of $dN$ and $dR$ are proportional not only to the values of the nucleation frequency $I$ and crystal growth rate $u$, but also to the relative amount of the mother phase $x_m$ per unit volume, *i.e.*, can be calculated using ratios:

$$dN = x_m I dt, \tag{5}$$

$$dR = x_m u dt. \tag{6}$$

In equation (5), the factor $x_m$ means that new crystallization centres arise only in that part of the volume that has not undergone the conversion. This statement is obvious, due to which relation (5) is traditionally used in studies of crystallization kinetics of materials from liquid and amorphous states [55, 56].

Turning to the growth processes analysis, the author [54] states that at the stage of mass crystallization, each individual crystal can grow only in those directions in which it borders with the mother phase. The probability of the existence of growth directions that are not blocked by neighbouring crystals decreases as the fraction of the transformed volume $x = 1 - x_m$ increases, tending to zero as $x \to 1$. On the contrary, at the very early stages of solidification, when $x$ is negligible, $x_m \approx 1$ and, therefore, crystals grow freely with a rate $u$, which is determined by the temperature and the mechanism of the process. The noted features of the joint growth of many crystals are taken into account by the form of Eq. (6), which gives reason to use it as the second basic relation of the kinetic model [54].

As can be seen from Eqs. (5) and (6), in accordance with the considered version of the kinetic model, the formation of new crystallization centres and an increase in crystal size cease when one of the two conditions are met:

• if $I \to 0$ and $u \to 0$, which occurs during deep supercooling of the melt and precedes to its amorphization;

• in case of complete exhaustion of the maternal phase ($x_m \to 0$), which indicates the completion of the transformation (in this case, the parameters $I$ and $u$ can have sufficiently large numerical values).

It follows that the parameters $I$ and $u$ included in Eqs. (5) and (6) characterize only the potential possibilities of the nucleation and crystal growth processes, while the actual kinetic behaviour of these processes is determined by the effective parameters:

$$I_{\text{eff}} = (1 - x) I, \tag{7}$$

$$u_{\text{eff}} = (1 - x) u. \tag{8}$$

Taking into account relations (7) and (8), the principle of modelling of mass crystallization kinetics proposed in [54] is called the approximation of the effective rates of nucleation and crystal growth.

Application of this approximation removes the restrictions inherent in Eq. (4) regarding the prediction of growth kinetics, *i.e.*, allows calculating the characteristic scales of crystals in rapidly quenched materials and thereby provides an additional (besides $\upsilon_c$ magnitude) quantitative criterion for comparing the results of model studies with the corresponding experimental data. Another advantage of the model [54] is the possibility of using it for complex transformations with competition of several crystalline phases and crystallization mechanisms. In the framework of approximation [54], mathematical models of the structure formation processes under conditions of rapid cooling of melts on a heat-conducting substrate, casting into a metal mould, and laser processing with surface melting were constructed. In particular, the effect of compositional and technological factors on the microstructure parameters of the QLS products and the glass-forming ability of materials was studied using the kinetic equation of single-phase crystallization [4, 7, 8, 50, 57], obtained from the basic relations (5)–(8):

$$x(t) = \frac{4}{3}\pi \int_{t_m}^{t} (1 - x(t'))I(t') \left[ R_c(t') + \int_{t'}^{t} (1 - x(t''))u(t'')dt'' \right]^3 dt', \qquad (9)$$

where $t_m$ — time to reach the melting temperature of the melt; $t$, $t'$, $t''$ — current time points $t_m \le t' \le t'' \le t \le t_e$ ($t_e$ — transformation end time).

According to the results of this block of calculations for completely crystallisable materials, the dependences of the most probable crystal sizes on the cooling rate of the QLS products are constructed. For materials with significantly different glass-forming ability, the values of the critical thickness $l_c$ and the cooling rate $\upsilon_c$ of the melt layers, which provide the structure of metal glasses, are determined. For all controlled parameters, agreement between the calculated and experimental data is achieved.

The possibility of using the approximation [54] for the computational analysis of the crystallization kinetics of several competing phases is illustrated by the example of the effect of the formation of the metastable cerium polytype (μ-Ce). According to the data of [58, 59], in the structure of rapidly quenched foils of this metal a mixture of f.c.c. γ-Ce with a metastable μ-modification having a seven-layer hexagonal compact lattice with a sequence of stacking close-packed atomic layers of the type of *ABACABC*… is fixed. It is concluded that the μ-Ce structure is formed as a result of the accumulation and ordered arrangement of interstitial packing defects ($PD_+$) in the equilibrium γ-modification lattice, which leads crystallization under conditions of rapid melt cooling.

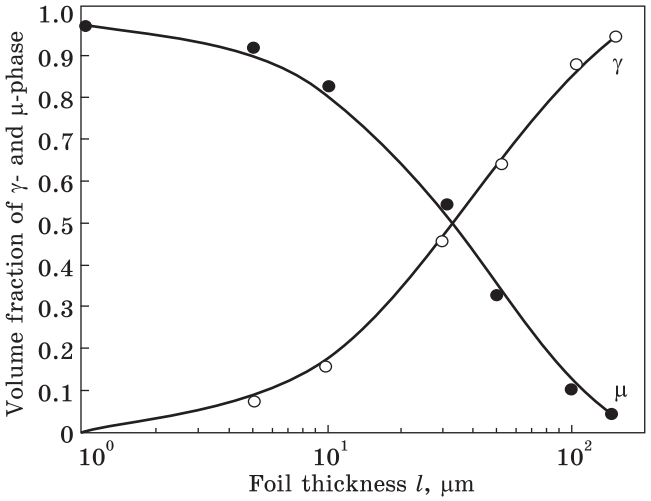


*Fig. 4.* Changes in the relative amounts of the equilibrium (γ) and metastable (μ) cerium polytypes depending on the thickness of rapidly quenched foils [60]

Based on relations (5)–(8) and conclusions on the proposed mechanism of μ-Ce formation, kinetic equations for calculating the relative amounts of equilibrium ($x_\gamma$) and metastable ($x_\mu$) cerium modifications were obtained in [60] as follow:

$$x_\gamma(t) = \frac{4}{3}\pi \int_{t_\mu}^{t} x_\mu(t')(1-q_\mu) I_\gamma(t') \left[ R_c^\gamma(t') + \int_{t'}^{t} x_\mu(t'') u_\gamma(t'') dt'' \right]^3 dt', \quad (10)$$

$$x_\mu(t) = \frac{4}{3}\pi \int_{t_\mu}^{t} x_\mu(t') q_\mu I_\gamma(t') \left[ R_c^\gamma(t') + \int_{t'}^{t} x_\mu(t'') u_\gamma(t'') dt'' \right]^3 dt', \quad (11)$$

where $q_\mu$ is the probability of crystal lattice transformation γ-Ce → μ-Ce.

The $q_\mu$ value was correlated with the concentration of $PD_+$, assuming that it increases with an increase in the cooling rate or a decrease in the thickness $l$ of the QLS products. To formalize this dependence, we used the relation:

$$q_\mu = \exp(-l/l_{cr}), \quad (12)$$

where $l_{cr}$ is the experimentally determined critical thickness of rapidly quenched foils, the excess of which makes the formation of μ-Ce unlikely.

Using equations (10)–(12), the authors of [60] performed a numerical analysis of the crystallization kinetics of thin (1–150 μm) Ce-layers that solidify on a copper quenching block. It was shown that with an increase in the thickness of rapidly quenched foils, the relative amount of metastable modification $x_\mu^e$ decreases from 0.98 to ≈0.06 (Fig. 4). Approximate equality of values $x_\mu^e$ and $x_\gamma^e$ is achieved in layers ≈35 μm thick, which is consistent with the results of x-ray phase analysis.

Among the complex transformations of a competitive type, it is also the crystallization of the molten bath formed during the interaction of laser radiation with the surface of the material. According to the structural studies [61], two zones are revealed in the cross sections of the melted layers, one of which is formed as a result of the growth of crystals located on the fusion boundary into the melt, and the second one, by nucleation and growth of new crystallization centres in the part of the laser bath located above the front of matrix crystals (FMC). The solidification process begins with the growth of matrix crystals, and the conditions for the emergence of new centres are created after a certain time interval, as the overlying layers of the melt become supercooled [62]. At the stage of joint development of two competing mechanisms, crystals growing from the bath bottom collide with newly nucleating crystals at the front, while the growth of the latter is additionally blocked due to mutual collisions of neighbouring particles.

As shown in Refs. [63, 64], the complex nature of the crystallization processes of a laser bath can be described using the approximation [54]. In the considered version of the model, the effective rates of nucleation and crystal growth are limited by the volume fraction of the mother phase $x'_m$ in the zone lying above the FMC, which is determined from the relation:

$$x'_m = \frac{1 - x_g - x_{ng}}{1 - x_g}, \tag{13}$$

where $x_g$ — volume fraction of the laser fusion zone occupied by crystals growing from the bath bottom; $x_{ng}$ — the converted volume fraction formed due to the implementation of the mechanism of new crystallization centres nucleation and growth.

Taking into account relation (13), kinetic equations corresponding to two competing mechanisms were obtained in the form [63]

$$x_g(t) = \frac{1}{h_0} \int_{t_m}^{t} \frac{1 - x_g(t') - x_{ng}(t')}{1 - x_g(t')} u_g(t')\, dt', \tag{14}$$

$$x_{ng}(t) = \frac{3}{4}\pi \int_{t_m}^{t} (1 - x_g(t') - x_{ng}(t'))\, I(t') \times \times \left[ R_c(t') + \int_{t'}^{t} \frac{1 - x_g(t'') - x_{ng}(t'')}{1 - x_g(t'')} u_{ng}(t'')\, dt'' \right]^3 dt', \tag{15}$$

where $h_0$ is initial depth of the fused zone; $u_g$, $u_{ng}$ are the rate of germination of matrix crystals into the melt and the rate of isotropic growth of newly nucleating crystals, respectively.

The total volume fraction of the laser-molten bath, crystallized at any given point in time $t \in [t_m, t_e]$ using two competing mechanisms, is

calculated by summing their relative contributions, *i.e.*,

$$x(t) = x_g(t) + x_{ng}(t). \quad (16)$$

Kinetic Eqs. (14)–(16) were solved in accordance with the heat equation:

$$C_p \rho \frac{\partial T}{\partial t} = k \frac{\partial^2 T}{\partial z^2} + \rho \frac{\Delta H_m}{M} \frac{\partial x}{\partial t}, \quad (17)$$

where $T$, $t$, $z$ are current values of temperature, time, and coordinates in the heat sink direction; $C_p$, $\rho$, $k$, $\Delta H_m$, $M$ are specific heat, density, thermal conductivity, molar heat of fusion, and molar mass of the processed material, respectively.

The presented mathematical model in Ref. [64] was used for the computational analysis of structure formation processes during solidification of the laser fusion zone of a massive nickel plate. The laser-bath depth $h_0$ was varied by changing the laser-pulse duration $\tau$ and the radiation-power density $q$, which is absorbed by the surface.

It was shown that when the plate is melted by laser pulses of duration $\tau = 10^{-3}$ s to a depth $h_0$ of 18 to 85 μm, the crystallization of the bath occurs solely due to the 'g-mechanism', *i.e.*, by promotion of the front of matrix crystals into the melt. At reducing the pulse duration to $\tau = 0.5 \cdot 10^{-7}$ s, the competitiveness of the nucleation and growth of new crystals mechanism increases, and the maximum contribution of this mechanism to the total fraction of the crystallized volume $x_e$ reaches $\approx 0.47$ at $h_0 = 170$ nm.

## 4. Thermokinetic Analysis of the Conditions for the Formation of Metal Glasses

As noted above, in the kinetic approach to the problem of metals' and alloys' amorphization, conditions under which only a negligible fraction of the studied volume $x_e$ ($10^{-2}$ or $10^{-6}$) crystallizes over the entire cooling time of the melt, are analysed. The main result of kinetic studies of the tendency of materials to noncrystalline solidify are values of critical cooling rate $\upsilon_c$ (or melt layer thickness $l_c$), which provide a predetermined value $x_e$. The values $\upsilon_c$ calculated by using the TTT diagrams or by a consistent solution of the heat conduction and crystallization kinetics equations, as a rule, are in satisfactory agreement with the corresponding experimental estimates. However, these values separately do not provide an answer to the question of which parameters included in the kinetic equations $x(t)$ are responsible for the melts tendency to transition into the amorphous state. Considering this in [65, 66], a new version of the analysis of the conditions for the production of metal glasses was proposed. It reflects both the thermal and kinetic aspects of the process under study, and for this reason can be called thermokinetic.

The objects of the study were materials of four groups with a significantly different tendency to glass formation:

• metals (Al, Cu), which crystallize at all cooling rates achievable by modern methods of quenching from liquid state (up to ~$10^{11}$ K/s);

• metals (Ni, Ge), which transform into an amorphous state under extreme conditions of melt cooling in layers of submicron thickness [67, 68];

• metal–metalloid alloys ($Fe_{80}B_{20}$, $Fe_{40}Ni_{40}P_{14}B_6$) obtained in the form of amorphous ribbons with a thickness of 15–60 μm by melt spinning [69, 70];

• alloys based on magnesium and zirconium ($Mg_{65}Cu_{25}Y_{10}$, $Zr_{41.2}Ti_{13.8}Cu_{12.5}Ni_{10}Be_{22.5}$), which are amorphized by casting into a metal mould in sections of more than 1 mm [18].

The proposed approach is based on the results of model calculations of the dependences $T(t)$ and $x(t)$ [4]. At the moment of establishing a balance between the heat flux removed to the substrate and the flux released during crystallization, when the $T(t)$ curves pass through minimum point ($\partial T/\partial t = 0$), the fraction of the crystallized volume is about $10^{-2}$. Therefore, to obtain the same or even smaller relative amount of the crystalline phase in the structure of the hardening material, it is necessary and sufficient that the first derivative $\partial T/\partial t$ should keep a negative value over the entire time range $t_m - t_e$. In other words, the thermal criterion for melts amorphization is the condition:

$$\partial T/\partial t < 0. \qquad (18)$$

Combining inequality (18) with the heat equation for the melt (17), the amorphization condition was transformed to a form that allows the analysis to be extended to factors controlling the transformation kinetics [66]:

$$\upsilon_+ < |\upsilon_-|, \qquad (19)$$

where $\upsilon_+ = (\Delta H_m/MC_p)(\partial x/\partial t)$ is the heating rate due to the release of latent heat of transformation, $\upsilon_- = a(\partial^2 T/\partial z^2)$ is the cooling rate due to heat removal to the substrate, $a = k/(C_p\rho)$ is the coefficient of the melt thermal diffusivity.

An analysis of the dependences $\upsilon_+(t)$ and $|\upsilon_-(t)|$ shows that, to fulfil condition (19), the point $t_{\max}$ is critical. In this point, the crystallization rate $\dot{x} = \partial x/\partial t$ reaches its maximum value. It follows that to determine the possibility of noncrystalline solidification of the melt, it is sufficient to verify the feasibility of the relation:

$$\upsilon_+^m < |\upsilon_-^m| \text{ or } \left(\frac{\Delta H_m}{MC_p}\frac{\partial x}{\partial t}\right)\Bigg|_{t=t_{\max}} < \left|a\frac{\partial^2 T}{\partial z^2}\right|_{t=t_{\max}}. \qquad (20)$$

As an example, Fig. 5 shows the calculated dependences $\upsilon_+^m(l)$ and $|\upsilon_-^m(l)|$ for the melt layers of metals of the first (Al) and second (Ni)

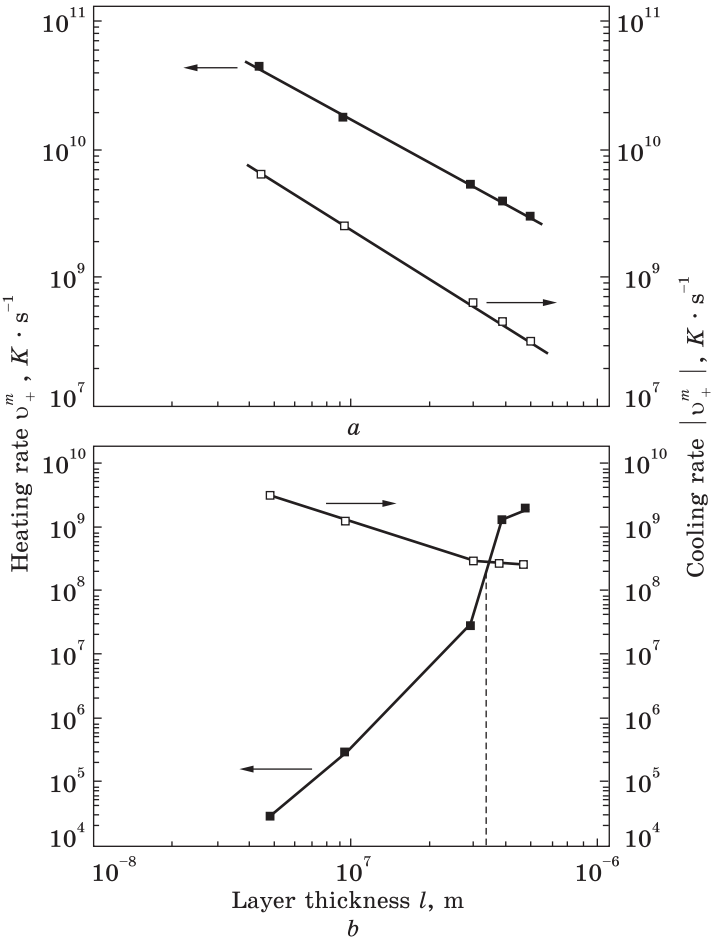


*Fig. 5.* Calculated dependences of the $\upsilon_+^m$ and $|\upsilon_-^m|$ parameters on the layer thickness of Al (*a*) and Ni (*b*) melts **[66]**

groups. It can be seen that for aluminium in the entire studied range of values (from 0.05 to 0.5 μm), the heating rate due to the release of latent heat of crystallization significantly exceeds the cooling rate due to heat removal to the substrate (Fig. 5, *a*). Therefore, the hardening of Al melt layers with a thickness $l \geq 0.05$ μm is accompanied by a recalescence effect, which is a thermal sign of complete crystallization.

In contrast to Al, for the Ni melt layers, the analysed dependences have a qualitatively different form (Fig. 5, *b*). In the region of small thicknesses, the cooling process prevails over the self-heating process, which indicates the fulfilment of the amorphization condition (20). With increasing $l$, the cooling slows down, while the heating rate, on the contrary, increases sharply. As a result, for some critical value $l = l_c$, the curves $\upsilon_+^m(l)$ and $|\upsilon_-^m(l)|$ intersects. For all $l > l_c$, the ratio of the analysed parameters changes to the opposite ($\upsilon_+^m(l) > |\upsilon_-^m(l)|$).Thus, the point $l_c$ separates the interval of thicknesses $l \leq l_c$, in which the nickel melt

solidifies in the glassy form, from the interval $l > l_c$ corresponding to the formation of fully crystallized structures. The critical cooling rate for Ni calculated from $l_c$ value is $\upsilon_c \approx 9 \cdot 10^9$ K/s, which practically coincides with the corresponding experimental estimate [67].

By further detailed analysis of the factors included in relation (20) was revealed that its variations are mainly determined by the maximum value of the crystallization rate $\dot{x}_m = \partial x/\partial t|_{t=t_{\max}}$. On the other hand, it was shown that for all the materials studied, a correlation of numerical values $\dot{x}_m$ and crystal growth rate $u(t_{\max})$ is observed. From here, it follows the key conclusion of the work regarding the fact that it is the crystal growth rate has a decisive influence on the $\dot{x}_m$ magnitude, and, consequently, on the tendency of melts to noncrystalline solidification. It is important that this conclusion was obtained not from general considerations, but by a consistent computational analysis of the relationships between heat transfer and crystallization.

Based on the thesis about the predominant role of the growth rate in increasing of the crystallized volume fraction, authors [66] explain the physical reasonability of using a quantitative criterion for the glass forming ability of materials. The role of a criterion plays a ratio of the difference between the free energies of the liquid and crystalline phases to the melt viscosity ($\Delta G_V/\eta$) calculated at a time $t_{\max}$. A decrease in this parameter slows down the growth processes, which increases the probability of noncrystalline solidification. To simplify the dimension of the proposed criterion, the difference in free energies per unit volume $\Delta G_V$ was used in the paper mentioned above. In this case, the ratio $\Delta G_V/\eta$ acquires the frequency dimension [$s^{-1}$].

The results of calculating the ratio $\Delta G_V/\eta$ showed that for the studied metals of the first group (Al, Cu), the desired value is ~$10^{10}$–$10^{11}$ $s^{-1}$ (Table 1). Since the metals under consideration crystallize completely even at extremely high melt cooling rates (~$10^{11}$ K/s), the given values

*Table 1.* **Calculated values of the $\Delta G_V/\eta$ criterion and parameters $l_c$ and $u(T_{\max})$ for materials with different glass-forming ability [66]**

| Group | Material | $l$, μm | $x_e$ | $T_{\max}$, K | $u(T_{\max})$, m/s | $\Delta G_V/\eta$, $s^{-1}$ |
|---|---|---|---|---|---|---|
| 1 | Al | 0.05 | 0.99 | 792 | 6.3 | $8.6 \cdot 10^{10}$ |
| | Cu | 0.05 | 0.99 | 1025 | 3.0 | $4.7 \cdot 10^{10}$ |
| 2 | Ni | 0.05 | $3 \cdot 10^{-6}$ | 890 | $1.6 \cdot 10^{-1}$ | $3.1 \cdot 10^{9}$ |
| | Ge | 0.15 | $2 \cdot 10^{-6}$ | 899 | $1.9 \cdot 10^{-2}$ | $2.1 \cdot 10^{8}$ |
| 3 | $Fe_{80}B_{20}$ | 12 | $4 \cdot 10^{-6}$ | 1027 | $4 \cdot 10^{-3}$ | $2.1 \cdot 10^{7}$ |
| | $Fe_{40}Ni_{40}P_{14}B_6$ | $8 \cdot 10^{2}$ | $2 \cdot 10^{-6}$ | 858 | $9 \cdot 10^{-6}$ | $6.6 \cdot 10^{5}$ |
| 4 | $Mg_{65}Cu_{25}Y_{10}$ | $4 \cdot 10^{3}$ | ~$10^{-6}$ | 580 | $10^{-5}$ | $1.6 \cdot 10^{5}$ |
| | $Zr_{41.2}Ti_{13.8}Cu_{12.5}Ni_{10}Be_{22.5}$ | $5 \cdot 10^{4}$ | ~$10^{-6}$ | 850 | $4 \cdot 10^{-6}$ | $3.1 \cdot 10^{4}$ |

$\Delta G_V/\eta$ characterize the conditions under which the effect of amorphization of metals is impossible.

For metals of the second group (Ni, Ge), the values of the $\Delta G_V/\eta$ criterion occupy the interval ~$10^8$–$10^9$ $s^{-1}$, which can be considered as a measure of the GFA of one-component melts, which are amorphized in the thinnest (<1 μm) sections of rapidly quenched foils.

The Fe-based alloys presented in Table 1 as materials of the third group, have a higher tendency to noncrystalline solidification compared to pure metals and, at the same time, significantly different. The values $\Delta G_V/\eta$ calculated for these alloys limits a rather wide range (≈$7 \cdot 10^5$–$2 \cdot 10^7$ $s^{-1}$), which also includes many other alloys that are amorphized upon quenching from the liquid state in sections $l_c$ from 10 to 800 μm.

The lowest level of the $\Delta G_V/\eta$ criterion (~$10^4$–$10^5$ $s^{-1}$) was recorded by calculations for bulk-amorphized alloys of the fourth group (Table 1), in which the structures of metal glasses are fixed under the conditions of obtaining castings with a thickness of 4–50 mm.

An analysis of the relationship of the $\Delta G_V/\eta$ criterion with the parameters $l_c$ and $u(T_{\max})$, which control the thermal regime and crystallization kinetics of melts, shows that the amorphizing materials studied in [66] have the range of $\Delta G_V/\eta \approx 10^4$–$10^{10}$ $s^{-1}$. Consequently, from the kinetic point of view, the different tendency of metal melts to noncrystalline solidification can be explained by the difference in the crystal growth rates at a temperature $T_{\max}$. The quantitative criterion defining the quantity $u(t_{\max})$ is the ratio $\Delta G_V/\eta$. The critical value of this parameter, which separates the glassy materials from materials that do not exhibit such a capacity under any physically correct melt cooling conditions, is ~$10^{10}$ $s^{-1}$, which corresponds to $u(T_{\max}) \approx 1$ m/s.

As the parameter $\Delta G_V/\eta$ decreases, the tendency of materials to noncrystalline solidification increases and, starting from values ~$10^6$ $s^{-1}$ ($u(T_{\max}) \approx 10^{-5}$ m/s), they acquire the ability to bulk amorphization. The intermediate region between the indicated limit values of the parameters $\Delta G_V/\eta$ and $u(T_{\max})$ is occupied by a wide range of materials of the second and third groups, which are obtained in the amorphous state by the known methods of rapid cooling of the melt on the heat-conducting substrates.

In conclusion, we note that the parameter values $u(T_{\max})$ and $l_c$ given in Table 1, are the main result of the version of the thermokinetic analysis of the metal melts glassy solidification conditions proposed in Ref. [66]. The originality of the $\Delta G_V/\eta$ criterion is in reflecting the physical picture of the metal glasses formation, linking the glass-forming ability of materials with the thermal regime of the process and the crystal growth kinetics. Unfortunately, for using the $\Delta G_V/\eta$ criterion in order to predict the results of the QLS, there are difficulties due to the limited reference information on the temperature dependences of the $\Delta G_V$ and $\eta$ parameters for many known and newly created glassy

alloys. At the same time, the models developed for calculating the thermodynamic parameters [71–74] as well as theoretical and experimental estimates of the supercooled melts viscosity [17, 75–77], partially remove these limitations and expand the possibilities of applying the approach [66] in studies and manufacturing technologies for metal glasses of new classes.

## 5. Analysis of the Materials' Tendency to the Total Suppression of the Crystallization

As shown above, rapidly quenched amorphous alloys are the result of crystallization suppression and 'freezing' of the melt atomic configuration corresponding to the glass transition temperature $T_g$. In the model studies of these processes [7, 12, 13], the critical melt cooling rate $\upsilon_c$ at which only a negligible fraction of the crystalline phase $x_e$ is fixed per unit volume, which is commensurable with the sensitivity limits of transmission electron microscopy (~$10^{-6}$) or x-ray phase analysis (~$10^{-2}$), is determined. The $\upsilon_c$ value is calculated by a coordinated solution of the thermal and kinetic tasks for the melt layers that solidify in contact with a massive heat sink. It was shown [66] that the $\upsilon_c$ parameter characterizes the thermal regime under which the crystal growth processes are suppressed, while the action of the nucleation mechanism does not stop. Obviously, with an increasing of the cooling rate relatively $\upsilon_c$, the favourable conditions that will slow down the process of crystal nucleation should be created. The ultimate occurrence of this effect is the complete suppression of crystallization with the fixation of truly amorphous structures, which are devoid of inclusions of the crystalline phase.

In the only known example of a quantitative analysis of the conditions for the formation of such structures [78], an algorithm for calculating the critical cooling rate $\upsilon_c^*$, at which suppresses the crystal nucleation process, is proposed. The $\upsilon_c^*$ parameters for materials of different classes (oxides, molecular liquids, pure metals, *etc.*) are estimated. It is shown that, overall, the proposed method allows estimating the relative tendency of the studied substances to amorphization. However, both some assumptions used in calculating of the physical parameters of the model, and the obtained estimates of the $\upsilon_c^*$ value, in particular, concerning to pure metals, need to be clarified and verified. Indeed, according to the data of [78], for pure tin, the value $\upsilon_c^*$ is only ~$10^2$ K/s, although there is no information in the literature regarding the susceptibility of this metal to noncrystalline solidification.

To obtain more objective estimates of the complete-amorphization conditions for metal melts, authors of Refs. [79–81] used an improved algorithm for calculating the critical cooling rate $\upsilon_c^*$. At that point, no more than one crystalline nucleus is formed in a unit volume during the

passage of the temperature range $T_m$–$T_g$. Assuming a constant cooling rate for layers of a given thickness, the $\upsilon_c^*$ values were determined using the following basic relationship:

$$\frac{1}{\upsilon_c^*} \int_{T_g}^{T_m} I(T)\, dT \le 1. \qquad (21)$$

The calculations were performed for the same metals and alloys with different glass forming abilities, which were used in [66] when analysing the conditions for the formation of metal glasses. It is shown that the real perspective to complete suppression of crystallization with the possibility of experimental confirmation of the effect revealed by the calculations is provided only by bulk-amorphized alloys of the fourth group, which are based on Mg and Zr. The corresponding values $\upsilon_c^*$ are ~$10^7$ and ~$3 \cdot 10^4$ K/s. Such cooling rates can be achieved by the well-known QLS methods.

To develop the calculation algorithm [79–81], a combined model of amorphization of metal melts was proposed in [7]. It provides for the sequential determination of two critical parameters $\upsilon_c$ and $\upsilon_c^*$. This allows us to perform a comparative analysis of thermal conditions that ensure the formation of amorphous–nanocrystalline structures, characteristic for metal glasses and truly amorphous states without inclusions of 'frozen' crystallization centres.

Constructing a combined model of suppression crystallization, we proceeded from the fact that, as the cooling rate increases, the conditions for the growth processes ($\upsilon = \upsilon_c$, $x_e \approx 10^{-2}$) and then the nucleation of crystals ($\upsilon = \upsilon_c^*$, $N_e^V < 1$, where $N_e^V$ is the number of crystallization centres arising in the studied volume $V$ over the entire cooling time of the melt) become impossible. The results of two series of calculations are presented in Ref. [7]. In the calculations of first series, the critical values of the cooling rate $\upsilon_c$ and the thickness $l_c$ of the melt layers, at which the volume fraction of crystalline phase inclusions does not exceed the sensitivity limit of x-ray phase analysis (~$10^{-2}$), were determined. The calculations were carried out using the algorithm for the coordinated numerical solution of the kinetic equation (9) with one-dimensional differential heat equations for the melt and heat receiver [8, 57]. The values of the parameters $I$, $R_c$, $u$ included in relation (9) were determined using the formulas of the classical crystallization theory [82] under the assumption of homogeneous nucleation and normal crystal growth mechanisms.

In the second block of calculations for the melt layers of thickness $l < l_c$, we determined the number of crystalline nuclei $N_e^V$ that form upon cooling from $T_m$ to $T_g$ in a given volume $V = Sl$, where $S = 10^4$ m$^2$ is the surface area of plane-parallel samples used in structural studies. For

this purpose, we used the ratio:

$$N_e^V = Sl\int \frac{I(T)}{\upsilon(T)}dT\,. \tag{22}$$

In calculating of dependences $I(T)$, we took into account the correction of the nonstationary nature of distribution of heterophase fluctuations in size under conditions of the melts rapid cooling [78]:

$$I(T) = I_0(T)\exp(-\tau/t), \tag{23}$$

$$I_0(T) = \frac{N_a D(T)}{a_0^2}\exp\left(-\frac{16}{3}\pi\frac{V_m^2\sigma^3}{\Delta G_m^2(T)\,k_B T}\right), \tag{24}$$

$$\tau = \frac{\pi V_m^2\sigma^2}{D(T)\Delta G_m^2(T)}, \tag{25}$$

$$t = \int_T^{T_m}\frac{dT}{\upsilon(T)}, \tag{26}$$

where $I_0$ is a stationary frequency of crystallization centres formation, $\tau$ is a delay time when establishing a stationary size distribution of subcritical nuclei, $t$ is a cooling time of the melt from $T_m$ to $T$, $N_a$ is a number of atoms per unit volume, $D$ is a diffusion coefficient of atoms at the melt–crystal interface, $a_0$ is an interface thickness (atomic diameter), $V_m$ is a molar volume, $\sigma$ is a specific free energy of the crystal surface, and $\Delta G_m$ is a molar difference of free energies of liquid and crystalline phases.

The diffusion coefficient was expressed through the dynamic viscosity of the melt $\eta$ using the Stokes–Einstein relation:

$$D(T) = \frac{k_B T}{3\pi a_0\eta(T)}. \tag{27}$$

Taking into account Eqs. (23)–(27), Eq. (22) can be presented in the form:

$$N_e^V = V\int_{T_g}^{T_m}\frac{K_1 T}{\eta(T)\,\upsilon(T)}\exp\left(-\frac{K_2}{T\Delta G_m^2(T)}\right)\exp\left(-\frac{K_3\eta(T)}{T\Delta G_m^2(T)\,t}\right)dT, \tag{28}$$

where

$$K_1 = \frac{N_a k_B}{3\pi a_0^3}, \tag{29}$$

$$K_2 = \frac{16\pi V_m^2\sigma^3}{3k_B}, \tag{30}$$

$$K_3 = \frac{3\pi^2 a_0 V_m^2\sigma^2}{k_B}. \tag{31}$$

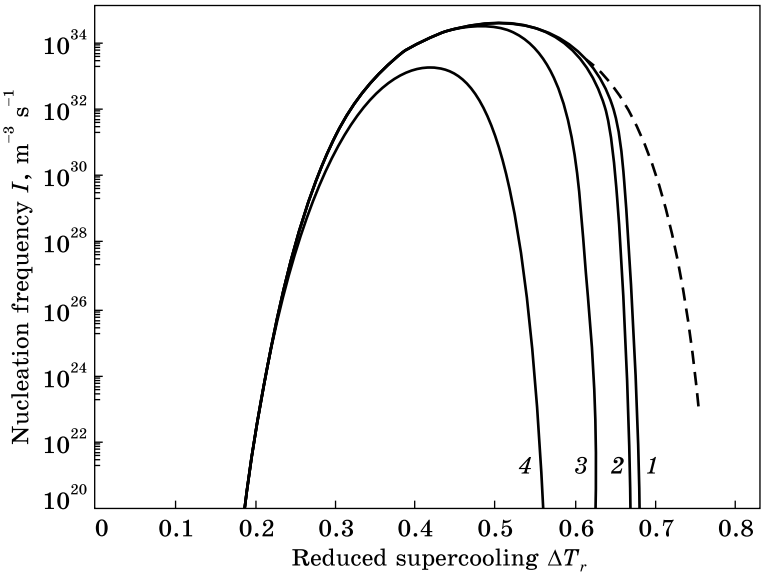


*Fig. 6.* Dependences of the stationary $I_0$ (dashed) and nonstationary $I$ (solid lines) nucleation frequencies on the reduced supercooling $\Delta T_r$ for Ni layers quenched from the liquid state with cooling rates $\upsilon \geq \upsilon_c$: $1.7 \cdot 10^9$ K/s (*1*), $5.5 \cdot 10^9$ K/s (*2*), $1.1 \cdot 10^{11}$ K/s (*3*), and $2.3 \cdot 10^{12}$ K/s (*4*) [7]

As a quantitative characteristic of the tendency of materials to the nucleation process suppression, the authors of [7] considered the critical thickness of the melt layer $l_c^*$, which ensures the fulfilment of inequality $N_e^V < 1$. The critical cooling rate $\upsilon_c^*$, which corresponds to this thickness, was determined by a joint analysis of the dependences $\upsilon(T)$ and $I(T)$, giving to $\upsilon_c^*$ parameter the value of the function $\upsilon(T)$ at the temperature of the maximum nucleation frequency.

The results of calculations of critical parameters $l_c$, $\upsilon_c$, $l_c^*$, $\upsilon_c^*$ in a generalized form are presented in Table 2. As one can see, the values $l_c$

*Table 2.* **Calculated values of the critical parameters providing the formation of metallic glasses ($l_c$, $\upsilon_c$) and truly amorphous ($l_c^*$, $\upsilon_c^*$) structures [7]**

| Material | Thickness (μm) and cooling rate (K/s) of melt layers | | | | | |
|---|---|---|---|---|---|---|
| | $l_c$ | $l_c^{\exp}$ | $\upsilon_c$ | $\upsilon_c^{\exp}$ | $l_c^*$ | $\upsilon_c^*$ |
| Ni | 0.25 | <1 [67] | $1.7 \cdot 10^9$ | ~$10^{10}$ [67] | – | – |
| $Fe_{80}B_{20}$ | 43 | 40 [13] | $5.5 \cdot 10^5$ | $6.5 \cdot 10^5$ [13] | 0.09 | $6.3 \cdot 10^9$ |
| $Mg_{65}Cu_{25}Y_{10}$ | $7.4 \cdot 10^3$ | $4 \cdot 10^3$ [84]<br>$7 \cdot 10^3$ [83] | 34 | 50 [84] | 10 | $1.3 \cdot 10^7$ |
| $Zr_{41.2}Ti_{13.8}Cu_{12.5}Ni_{10}Be_{22.5}$ | $5 \cdot 10^4$ | $5 \cdot 10^4$ [84] | 1.3 | 1.0 [84]<br>1.8 [46] | 550 | $2.7 \cdot 10^3$ |

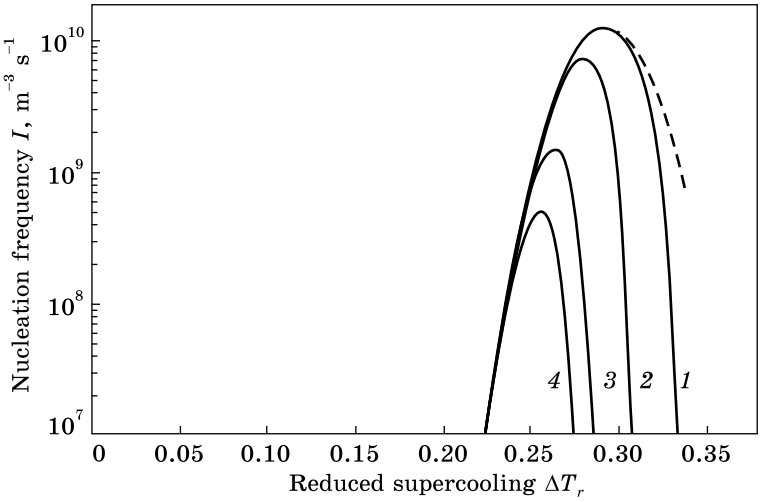


*Fig. 7.* Dependences of the $I_0\Delta(T_r)$ (dashed line) and $I\Delta(T_r)$ (solid lines) for the $Zr_{41.2}Ti_{13.8}Cu_{12.5}Ni_{10}Be_{22.5}$ alloy layers quenched from the liquid state with cooling rates $\upsilon \geq \upsilon_c$: 1.3 K/s (*1*), 64.4 K/s (*2*), $9.8 \cdot 10^{-2}$ K/s (*3*), and $2.7 \cdot 10^{3}$ K/s (*4*) [7]

and $\upsilon_c$ determined by the results of the first block of model calculations are consistent with the experimental estimates given in the literature, which indicates the adequacy of the mathematical model used in [7] (along with other mathematical models [85]) and the correctness of the calculated data obtained with its help.

According to the values of the critical thickness $l_c^*$ and cooling rate $\upsilon_c^*$ of the melt layers, which are presented in the Table 2, the fundamental possibility of complete suppression of crystallization processes demonstrate only materials with medium and high levels of GFA. This possibility appears in the $Fe_{80}B_{20}$ alloy only under extreme conditions of QLS ($l_c^* \approx 0.1$ μm, $\upsilon_c^* \approx 10^{10}$ K/s), the guaranteed providing of which is problematic. For the bulk-amorphized Mg- and Zr-based alloys, the critical values of the analysed parameters (10 μm, ~$10^7$ K/s and 550 μm, ~$3 \cdot 10^3$ K/s, respectively) can be achieved by traditionally used QLS methods, such as melt spinning and casting into a metal mould.

In the final section of Ref. [7], an analysis of factors, which control the nucleation kinetics under conditions of melts rapid cooling, was made. For this purpose, according to Eqs. (23)–(26), the dependences of the frequency of stationary ($I_0$) and non-stationary ($I$) nucleation on reduced supercooling of the melt $\Delta T_r$ were calculated. The dependences $I(\Delta T_r)$ were calculated for various cooling rates $\upsilon_c \leq \upsilon \leq \upsilon_c^*$. Calculated results for materials with a minimum (Ni) and maximum (Zr-based alloy) glass forming ability are shown in Figs. 6 and 7.

As can be seen from the graphs $I_0(\Delta T_r)$, the compared materials are characterized by radically different values of the maximum of statio-

nary nucleation frequency $I_0^{\max}$ and the corresponding supercoolings $\Delta T_r^{\max}$ of the melt. For Ni, the analysed parameters are, respectively, $\approx 4 \cdot 10^{34}$ m$^{-3}\cdot$ s$^{-1}$ and 0.49, while, for the Zr-alloy, their values decrease to ~$10^{10}$ m$^{-3}\cdot$ s$^{-1}$ and 0.29. An analysis of the dependences $I_0(\Delta T_r)$ for all the materials studied in [7] leads to the conclusion that one of the probable reasons for the impossibility of obtaining pure metals in a truly amorphous state is the very high (>$10^{29}$ m$^{-3}\cdot$s$^{-1}$) values of $I_0^{\max}$ parameter.

It is also important that the maximum values of stationary nucleation frequency are achieved with deep ($(0.44–0.49)T_m$) supercoolings of single-component melts. This increases the length of the period of high-speed crystallization centres formation and, therefore, reduces the probability of noncrystalline solidification of metals.

In the framework of the discussed above argument, which relates the tendency of materials to form truly amorphous structures with parameters $I_0^{\max}$ and $\Delta T_r^{\max}$, the bulk-amorphized alloys, due to incomparably lower values $I_0^{\max}$ in comparison with pure metals and a shift of $I_0(\Delta T_r)$ dependences to lower reduced supercoolings, are among the materials most prone to complete crystallization suppression. Nevertheless, according to the calculated data, even the lowest parameter values $I_0^{\max} = 10^{10}$ m$^{-3}\cdot$ s$^{-1}$ and $\Delta T_r^{\max} = 0.29$ for the five-component Zr-based alloy analysed in [7] do not provide structures without inclusions of quenching nuclei.

The second important factor, which controls the tendency of materials to completely crystallization suppression, is the sensitivity of the crystal nucleation kinetics, which is due to the nonstationary nature of the processes of crystalline nuclei formation upon quenching from a liquid state to the melt cooling mode. To illustrate the effectiveness of this criterion in [7, 81], the dependences of the of nonstationary nucleation frequency on reduced supercooling $I(\Delta T_r)$ were calculated for various cooling rates of melts $\upsilon_c \le \upsilon \le \upsilon_c^*$ and were combined with graphs $I_0(\Delta T_r)$.

As seen from Figs. 6 and 7, with an increasing of the cooling rate, the maximum values of the nonstationary nucleation frequency are decreasing, the $I(\Delta T_r)$ graphs narrow and shift to a region of lower values $\Delta T_r$. The observed changes in the dependences $I(\Delta T_r)$ contribute to an increase in the probability of noncrystalline solidification of QLS products. However, in materials with low glass-forming ability, a tendency to slow down of nucleation processes is detected only at extremely high (>$10^{12}$ K/s) cooling rates (Fig. 6), which exceeds the limit level for the known QLS methods. Moreover, pure metals in the entire range of cooling rate variation retains high (>$10^{20}$ m$^{-3}\cdot$s$^{-1}$) values of the nucleation frequency, which makes it impossible to obtain truly amorphous states. On the contrary, for the Mg- and Zr-based bulk-amorphized alloys, the maximum of $I(\Delta T_r)$ dependences decreases to ~$10^8$–$10^{11}$ m$^{-3}\cdot$s$^{-1}$ (Fig. 7), which represents real conditions for nucleation processes suppressing.

## 6. Conclusions

A review of the literature data on the conditions for partial and complete suppression of crystallization during rapid cooling of metal melts is carried out.

The advantages and limitations of the thermodynamic, structural, physicochemical, and kinetic criteria used to predict the tendency of materials to noncrystalline solidification are considered. It is shown that the kinetic approach based on the algorithm for the consistent solution of the heat conduction equations and crystallization kinetics for thin melt layers hardening in contact with a massive heat receiver is the most universal and physically correct.

Examples of using of developed by the authors model of effective nucleation and crystal growth rates in computational studies of the complex transformations kinetics, in which several crystalline phases and/or crystallization mechanisms are competing, are presented.

The results of a computational analysis of the melting cooling regimes in which the total fraction of the crystallized volume does not exceed the sensitivity limit of transmission electron microscopy ($\sim 10^{-6}$) are presented. It is shown that the probability of the formation of amorphous–nanocrystalline structures typical to metal glasses is determined by the crystal growth rate, the value of which is controlled by the ratio of the difference between the free energies of the liquid phases, which are crystallizing $\Delta G_V$ and melt viscosity $\eta$. Estimations of the $\Delta G_V/\eta$ criterion are obtained for materials of four groups with significantly different glass-forming ability.

The literature data on the fundamental possibility and physical premises of the complete suppression of crystallization of metal melts are generalized. Evidence that under real conditions of QLS, true amorphous states can be obtained only in bulk-amorphized alloys that solidify in the form of metal glasses in cross sections of more than 1 mm is presented. It is concluded that the main factors increasing the tendency of melts to complete crystallization suppression are relatively low ($\leq 10^{20}$ $m^{-3} \cdot s^{-1}$) stationary nucleation frequencies, as well as the effect of the retardation of crystallization centres formation with increasing the cooling rate.

REFERENCES

1. W. Klement and R.H. Willens, *Nature*, **187**: 869 (1960). https://doi.org/10.1038/187869b0
2. M.E. McGenry, M.A. Willard, and D.E. Laughlin, *Progr. Mater. Sci.*, **44**, No. 4: 291 (1999). https://doi.org/10.1016/S0079-6425(99)00002-X
3. I.S. Miroshnichenko, *Izvestiya VUZov. Chernaya Metallurgiya*, **7**: 97 (1982) (in Russian).

4. A.B. Lysenko, G.V. Borisova, O.L. Kravets, and A.A. Lysenko, *Phys. Met. and Metallogr.*, **106**: 435 (2008).
https://doi.org/10.1134/S0031918X0811001X
5. A.B. Lysenko, O.L. Kravets, and G.V. Borisova, *Kharkiv NFTTS MON i NAN Ukrainy*, **2**: 369 (2009) (in Russian).
6. A.B. Lysenko, O.L. Kosynska, and D.G. Skipochka, *Visnyk Dnipropetrovs'kogo Universytetu. Seriya: Fizyka. Radioelektronika*, **24**, No. 23: 75 (2016) (in Russian).
7. O.B. Lysenko, I.V. Zagorulko, T.V. Kalinina, and N.O. Kugai, *Metallofiz. Noveishie Tekhnol.*, **40**, No. 1: 1 (2018) (in Russian).
https://doi.org/10.15407/mfint.40.01.0001
8. A.B. Lysenko, O.L. Kravets, and A.A. Lysenko, *Metallofiz. Noveishie Tekhnol.*, **30**, No. 3: 415 (2008) (in Russian).
9. N.F. Gadzyra, Ye.I. Khar'kov, and I.A. Yakubtsov, *Metallofizika*, **11**, No. 1: 88 (1989) (in Russian).
10. A.L. Greer, *Acta Metal.*, **30**: 171 (1982).
https://doi.org/10.1016/0001-6160(82)90056-6
11. J.Z. Jianga, J. Saida, H. Kato, T. Ohsuna, and A. Inoue, *Appl. Phys. Lett.*, **28**, No. 23: 4041 (2003).
https://doi.org/10.1063/1.1581001
12. R. Sellger, W. Loser, and G. Righter, *Mater. Sci. Eng.*, **97**, 203 (1988).
https://doi.org/10.1016/0025-5416(88)90042-0
13. V.I. Tkatch, S.N. Denisenko, and B.I. Selyakov, *Acta Metallurg. Mater.*, **43**, No. 6: 2485 (1995).
https://doi.org/10.1016/0956-7151(94)00413-7
14. A.M. Glezer and Ye.I. Permyakova, *Nanokristally, Zakalennyye iz Rasplava* [Nanocrystals Quenched from the Melt] (Moscow: Fizmatlit: 2012) (in Russian).
15. H.W. Yang, J. Gong, R.D. Li, and J.Q. Wang, *J. Non-Cryst. Solids*, **355**, Nos. 45–47: 2205 (2009).
https://doi.org/10.1016/j.jnoncrysol.2009.08.001
16. Yu.K. Kovneristyy, E.K. Osipov, and Ye.A. Trofimova, *Fiziko-Khimicheskie Osnovy Sozdaniya Amorfnykh Metallicheskikh Splavov* [Physical and Chemical Basis for the Formation of Amorphous Metallic Alloys] (Moscow: Nauka: 1983) (in Russian).
17. H.A. Davies, *Amorfnyye Metallicheskiye Splavy* [Amorphous Metallic Alloys] (Ed. F.E. Luborsky) (Moscow: Metallurgiya: 1987), p. 16 (Russian translation).
18. A. Inoue, *Acta Mater.*, **48**, No. 1: 279 (2000).
https://doi.org/10.1016/S1359-6454(99)00300-6
19. G.V. Borisova, *Issledovanie Struktury i Svoystv Zakalyonnykh iz Zhidkogo Sostoyaniya Splavov na Osnove RZM* [Study of the Structure and Properties of the Rare-Earth-Based Alloys Quenched from a Liquid State] (Disser. for Cand. Phys.-Math. Sci.) (Kiev: Institute for Metal Physics, A.S. Ukr.SSR: 1984) (in Russian).
20. S. Pang, T. Zhang, K. Asami, and A. Inoue, *Mater. Sci. Eng. A*, **375–377**: 368 (2004); idem, *Mater. Sci. Eng. A*, **392**, Nos. 1–2: 455 (2005).
https://doi.org/10.1016/j.msea.2003.10.152;
https://doi.org/10.1016/j.msea.2004.10.023
21. Y. Li, S.C. Wang, C.K. Ong, H.H. Hug, and T.T. Goh, *Scripta Mater.*, **36**, No. 7: 783 (1997).
https://doi.org/10.1016/S1359-6462(96)00448-4

22. Z.P. Lu and C.T. Lin, *Acta Mater*, **50**: 3501 (2002). https://doi.org/10.1016/S1359-6454(02)00166-0
23. T. Egami and Y. Waseda, *J. Non-Cryst. Solids*, **64**: 113 (1984). https://doi.org/10.1016/0022-3093(84)90210-2
24. O.N. Senkov and D.B. Miracle, *J. Non-Cryst. Solids*, **317**: 34 (2003). https://doi.org/10.1016/S0022-3093(02)01980-4
25. O.N. Senkov and J.M. Scott, *Scr. Mater.*, **50**: 440 (2004). https://doi.org/10.1016/j.scriptamat.2003.11.004
26. D.B. Miracle and O.N. Senkov, *J. Non-Cryst. Solids*, **319**: 174 (2003). https://doi.org/10.1016/S0022-3093(02)01917-8
27. D.B. Miracle, W.S. Sanders, and O.N. Senkov, *Philos. Mag.*, **83**, No. 20: 2409 (2003). https://doi.org/10.1080/1478643031000098828
28. A. Inoue, *Progr. Mater. Sci.*, **43**: 365 (1998). https://doi.org/10.1016/S0079-6425(98)00005-X
29. O.N. Senkov and J.M. Scott, *Mater. Lett.*, **58**: 1375 (2004). https://doi.org/10.1016/j.matlet.2003.09.030
30. A. Inoue, B.N. Shen, and C.T. Chang, *Acta Mater.*, **52**, No. 14: 4093 (2004). https://doi.org/10.1016/j.actamat.2004.05.022
31. Yu.A. Skakov, *MiTOM*, **10**: 3 (2000).
32. A.B. Lysenko, I.V. Zagorulko, T.V. Kalinina, and A.A. Lysenko, *Nanostrukturnoye Materialovedenie*, **1**: 58 (2015) (in Russian).
33. I.V. Zahorulko, *Formuvannya Metastabil'nykh Krystalichnykh, Umovno ta Istynno Amorfnykh Faz pry Shvydkomu Okholodzhenni Rozplaviv* [Formation of Metastable Crystalline, Conditionally and Truly Amorphous Structures under Rapid Cooling of Melts] (Diss. Cand. Phys.-Math. Sci.) (Dnipro: Oles Honchar Dnipro National University: 2017) (in Ukrainian).
34. A.F. Polesya and L.S. Slipchenko, *Izvestiya AN SSSR. Metally*, **6**: 173 (1973) (in Russian).
35. S.R. Nagel and Y. Tauk, *Zhidkie Metally* [Liquid Metals] (Moscow: Metallurgiya: 1980) (in Russian).
36. A. Takeuchi and A. Inoue, *Mater. Sci. Eng.*, **304–306**: 446 (2001). https://doi.org/10.1016/S0921-5093(00)01446-5
37. D. Wang, Y. Li, and B.B. Sun, *Appl. Phys. Lett.*, **84**, No. 20: 4029 (2004). https://doi.org/10.1063/1.1751219
38. N. Mattern, U. Kuhn, and A. Gerbert, *Scr. Mater.*, **53**, No. 3: 271 (2005). https://doi.org/10.1016/j.scriptamat.2005.04.018
39. A.A. Kundg, M. Ohnuma, T. Ohkubo, and K. Hono, *Acta Mater.*, **53**, No. 7: 2091 (2005). https://doi.org/10.1016/j.actamat.2005.01.022
40. D.S. Park, D.H. Kim, and W.T. Kim, *Appl. Phys. Lett.*, **86**, No. 6: 061907 (2005). https://doi.org/10.1063/1.1862790
41. I.W. Donald and H.A. Davies, *J. Non-Cryst. Solids*, **30**, No. 2: 77 (1978). https://doi.org/10.1016/0022-3093(78)90058-3
42. D.R. Uhlmann, *J. Non-Cryst. Solids*, **7**, No. 4: 337 (1972). https://doi.org/10.1016/0022-3093(72)90269-4
43. *Rapidly Quenched Metals* (Eds. S. Steeb and H. Warlimont) (North-Holland: Elsevier: 1985). https://doi.org/10.1016/B978-0-444-86939-5.X5001-5
44. R. Sellger and W. Loser, *Acta Metall.*, **34**, No. 5: 831 (1986). https://doi.org/10.1016/0001-6160(86)90057-X

45. H.W. Bergmann and H.U. Fritsch, *Metal Science*, **16**: 197 (1982). https://doi.org/10.1179/msc.1982.16.4.19
46. Y.J. Kim, R. Busch, and W.L. Johnson, *Appl. Phys. Lett.*, **68**, No. 8: 1057 (1996). https://doi.org/10.1063/1.116247
47. S. Mukherjee, J. Schroers, W.L. Johnson, and W.-K. Rhim, *Phys. Rev. Lett.*, **94**: 245501 (2005). https://doi.org/10.1103/PhysRevLett.94.245501
48. T. Zhang, X. Zhang, and W. Zhang, *Mater. Lett.*, **65**: 2257 (2011). https://doi.org/10.1016/j.matlet.2011.04.033
49. S.S. Vil'kovskiy, V.P. Naberezhnykh, and B.I. Selyakov, *Amorfnyye Metallicheskie Splavy* [Amorphous Metallic Alloys] (Moscow: Metallurgiya: 1983) (in Russian).
50. A.B. Lysenko, O.L. Kravets, and G.V. Borisova, *Fizika i Tekhnika Vysokikh Davleniy*, **17**, No. 3: 52 (2007) (in Russian).
51. A.N. Kolmogorov, *Izvestiya AN SSSR. Seriya Matematicheskaya*, **3**: 355 (1937) (in Russian).
52. V.Z. Belen'kiy, *Geometriko-Veroyatnostnyye Modeli Kristallizatsii* [Geometrical Probability Models of Crystallization] (Moscow: Nauka: 1980) (in Russian).
53. E. Pineda, T. Pradell, and D. Crespo, *J. Non-Cryst. Solids*, **287**, Nos. 1–3: 88 (2001). https://doi.org/10.1016/S0022-3093(01)00548-8
54. A.B. Lysenko, *Visnyk Dnipropetrovskoho Universytetu. Seriya: Fizyka. Radioelektronika*, **19**, No. 2: 3 (2011) (in Russian).
55. V.I. Tkach, *Fizika i Tekhnika Vysokikh Davleniy*, **8**, No. 4: 91 (1998) (in Russian).
56. S.G. Rassolov and V. I. Tkach, *Izvestiya RAN. Seriya Fizicheskaya*, **69**, No. 8: 1218 (2005) (in Russian).
57. O.B. Lysenko, O.L. Kosynska, S.V. Gubarev, and T.V. Kalinina, *Metallofiz. Noveishie Tekhnol.*, **36**, No. 10: 1411 (2014) (in Russian). https://doi.org/10.15407/mfint.36.10.1411
58. A.B. Lysenko, G.V. Borisova, and O.L. Kravets, *Fizika i Tekhnika Vysokikh Davleniy*, **15**, No. 2: 96 (2005) (in Russian).
59. A.B. Lysenko, G.V. Borisova, O.L. Kravets, and A.A. Lysenko, *Phys. Met. Metallogr.*, **101**: 484 (2006). https://doi.org/10.1134/S0031918X06050097
60. A.B. Lysenko, G.V. Borisova, O.L. Kravets, and A.A. Lysenko, *Phys. Met. Metallogr.*, **113**: 588 (2012). https://doi.org/10.1134/S0031918X12060099
61. A.B. Lysenko, *Fizika i Khimiya Obrabotki Materialov*, **2**: 25 (2001) (in Russian).
62. A.B. Lysenko, N.A. Korovina, and Ye.A. Yakunin, *Metallofiz. Noveishie Tekhnol.*, **27**, No. 4: 1503 (2005) (in Russian).
63. A.B. Lysenko, N.A. Korovina, and I.A. Pavluchenkov, *Proc. 2nd Int. Conf. Laser Technologies in Welding and Materials Proceeding (May 23–27, 2005, Katsiveli, Crimea, Ukraine)* (Kyiv: E. O. Paton Electric Welding Institute of the NAS of Ukraine: 2005), p. 85.
64. A.B. Lysenko, N.A. Savinskaya, and Ye.A. Yakunin, *Proc. V Int. Conf Mathematic Modelling and Information Technologies in Welding and Related Processes (25–28 May, 2010 Katsiveli, Crimea, Ukraine)* (Kyiv: E.O. Paton Electric Welding Institute of the NAS of Ukraine: 2010), p. 97.

65. A.B. Lysenko, O.L. Kravets, and A.A. Lysenko, *The 13th Int. Conf. on Rapidly Quenched and Metastable Materials (August 24–29, 2008, Dresden)* (Dresden: IFW: 2008), p. 72.
66. A.B. Lysenko, O.L. Kravets, and A.A. Lysenko, *Metallofiz. Noveishie Tekhnol.*, **31**, No. 10: 1311 (2009).
67. H.B. Davies and J.B. Hull, *J. Mater. Sci.*, **11**: 215 (1976). https://doi.org/10.1007/BF00551430
68. H.B. Davies and J.B. Hull, *Scr. Metall.*, **7**: 637 (1973). https://doi.org/10.1016/0036-9748(73)90227-5
69. L.A. Davies, R. Ray, C.P. Chou, and R.C. O'Handley, *Scr. Metall.*, **10**: 541 (1976). https://doi.org/10.1016/0036-9748(76)90257-X
70. D.E. Polk and H.S. Chen, *Alloy Digest*, **10**: 4 (1976).
71. H. Jones, *Mater. Lett.*, **53**, Nos. 4–5: 364 (2002). https://doi.org/10.1016/S0167-577X(01)00508-0
72. K. Mondal and B.S. Murty, *Mater. Sci. Eng. A*, **454–455**: 654 (2007). https://doi.org/10.1016/j.msea.2006.11.123
73. K. Mondal, U.K. Chatterjee, and B.S. Murty, *Appl. Phys. Lett.*, **83**, No. 4: 671 (2013). https://doi.org/10.1063/1.1595725
74. A.-H. Cai, H. Wang, and X.S. Li, *Mater. Sci. Eng. A*, **435–436**: 478 (2006). https://doi.org/10.1016/j.msea.2006.07.021
75. L. Battezzati and A.L. Greer, *Acta Metal.*, **37**, No. 7: 1791 (1989). https://doi.org/10.1016/0001-6160(89)90064-3
76. T.A. Wanink, R. Busch, A. Masuhr, and W.L. Johnson, *Acta Mater.*, **46**, No. 15: 5229 (1998). https://doi.org/10.1016/S1359-6454(98)00242-0
77. A. Feltz, *Amorfnyye i Stekloobraznyye Neorganicheskiye Tverdyye Tela* [Amorphous and Vitreous Inorganic Solids] (Moscow: Mir: 1986) (Russian translation).
78. J.C.A. Wreswijk, R.G. Gossink, and J.M. Stevels, *J. Non-Cryst. Solids*, **16**: 15 (1974). https://doi.org/10.1016/0022-3093(74)90065-9
79. A.B. Lysenko, I.V. Zagorulko, and O.L. Kosinskaya, *Abstr. III Int. Conf. HighMatTech (October 3–7, 2011, Kyiv)* (Kyiv: I.M. Frantsevych Institute for Problems of Materials Science: 2011), p. 103.
80. A.B. Lysenko, I.V. Zagorulko, and O.L. Kosynskaya, *Abstr. III Int. Conf. Modern Problems of Condensed Matter (October 10–13, 2012, Kyiv)* (Kyiv: Taras Shevchenko National University of Kyiv: 2012), p. 164.
81. A.B. Lysenko, I.V. Zagorulko, T.V. Kalinina, and A.A. Kazantseva, *Physics and Chemistry of Solid State*, **14**, No. 4: 886 (2013).
82. J.W. Christian, *The Theory of Transformations in Metals and Alloys* (Oxford: Elsevier: 2002). https://doi.org/10.1016/B978-0-08-044019-4.X5000-4
83. R. Busch, W. Lin, and W.L. Johnson, *J. Appl. Phys.*, **83**, No. 8: 4134 (1998). https://doi.org/10.1063/1.367167
84. Z.P. Lu, H. Tan, S.C. Ng, and Y. Li, *Scripta Mater.*, **42**, No. 7: 667 (2000). https://doi.org/10.1016/S1359-6462(99)00417-0
85. T.G. Jabbarov, O.A. Dyshin, M.B. Babanli, and I.I. Abbasov, *Usp. Fiz. Met.*, **20**, No. 4: 584 (2019). https://doi.org/10.15407/ufm.20.04.584

Received 23.07.2019;
in final version, 18.03.2020